



Dynamic Definition of Machine Tool Feed Drive Models in Advanced Machine Tools

George Constantin^(✉)

University Politehnica of Bucharest, Bucharest, Romania
george.constantin@icmas.eu

Abstract. Machine tools in actual construction, being related to the trend towards to machine tools of high productivity and increased precision and having in view the context of transition to Industry 4.0, have to be studied deeply in the stage of conception and also in that of exploiting. For both situations, the modeling and simulation of the machine tool regarded as a mechatronic system represent methods of analysis, assessment, and optimization for its improvement.

This work proposes the approaching the subject from the point of view of modeling and simulation of one assembly of the machine tool that proves one of the most sensitive kinematic structure responsible for the machine tool precision. The modeling, either Rigid Body Simulation, Digital Block Simulation, Finite Element Modeling or combinations types, implies a concrete and accurate definition of the dynamic parameters stiffness, damping, and friction.

Some mathematical approaches for determining these parameters are presented. Also, some product catalog values and relations coming from the engineering and research experience applied to feed drive components and also to the whole kinematic chain are given. Furthermore, some practical testing and calculation methods are presented.

Keywords: Machine tool · Feed drive · Modeling · Stiffness · Damping Friction · Dynamic definition · Simulation

1 General Aspects of Machine Tool Dynamics

The constant trend in the evolution of machine tools is the constant increase in speeds and accelerations [5]. Therefore, the study of the dynamic behavior of machine tools and flexibility of structural elements must be considered.

That is why the dynamic models of the axes or the entire machine tool play a very important role in sizing the components and also in designing the control system.

The general way of considering the structures of machine tools that is historically viewed is that of massiveness. Thus, the massive structure leads to the high structural stiffness necessary to reduce the deformations under the influence of the machining forces and the static weight of the machine structure and workpiece. The deformation of the structure, which can be considered as a deformation of the structural loop, leads to errors at the interface between the cutting edge of the tool and the workpiece.

Rigid structures of machine tools tend to transmit vibrations at higher frequencies than deformable (non-rigid) ones. But rigid structures with low internal or external damping will transmit the vibrations caused mainly by the processing process throughout the structure. The transmitted vibrations will cause the structure to vary over time, which can be amplified in the workpiece, if the vibrations have frequencies close to a natural frequency of the machine tool. Therefore, a very rigid machine tool is not associated with small deformations.

The solution of deformation compensation, deformations which could be variable over time that cannot be easily estimated, is to measure deformations and compensate them. This task is almost impossible at high frequencies.

In addition to the rigidity characteristics of a machine tool, its ability to dampen vibrations created or transmitted by high stiffness should be considered. The performance of the machine tool is influenced by the component materials. Internal damping is different for different materials. For example, steel, cast iron and granite have different damping characteristics [22].

Some materials or components could also have nonlinear damping features. It may very well dampen vibration for a short period of time and then increase or maintain high amplitude, etc. Considering all these, all concerned phenomena have to be investigated along with how great the influence of rigidity and damping of the machine tool on the entire behavior of the structure should be.

2 Estimated and Measurable Behavior of Machine Tool

Measurable behavior of a machine tool is a combination of the geometric, thermal, static and dynamic behaviors. The dynamic behavior influences directly the machined part quality being observable through a lot of effects, such as the tracking error, outrunning, self excited vibrations, cross-talk, etc. In general, there are some weak points (bottlenecks) belonging to machine tool structure that influences the dynamic errors in a machine tool. Their identification becomes an essential condition for the desired improvement.

A comprehensive study of the dynamic behavior should be achieved by different methods:

- determination of the frequency answer (natural vibration mode respectively) of the machine tool structure, determined by the mass distribution, stiffness and damping properties in guides and bearings, and also by the degree of structural elasticity (for large frequency ranges);
- experimental modal analysis regarding a set of principal forces, and the acceleration signal distributed on the entire structure;
- simulation models based on rigid bodies and model with finite elements;
- structure testing, including the control loop (control coefficients, acceleration and jerk settings), feed-forward, filters, dead time, measuring system, etc.;
- simulation of the actuating systems, including also the structural machine tool components;

- experiments: evaluation of the input signals, cross-talk measurements, subsequent FFT (Fast Fourier Transform) and cross-talk interpretation;
- stability measurements (process parameters);
- on-line measurements on a running machine tool;
- integration of the process model in a virtual structure.

Given the example of a feed kinematic chain that represents a basic sub model of a machine tool (Fig. 1), we can make some remarks [4]. The constructive variant can be directly from the electric motor rotor to the lead screw through a coupling. One can ascertain that the model consists of components with rotation and translation motions (last element of the drive), with mass properties (mass, mass center, moment of inertia), and also of elastic and damping elements that give the model the characteristic of *dynamic*.

There are many types of modeling used in machine tool. The most developed and used modeling types are Rigid Bodies Simulation – RBS, Digital Block Simulation – DBS, and Finite Element Modeling – FEM. These techniques can be combined [3, 6–8, 29] for obtaining more accurate results in machine tool analysis. All techniques require the dynamic definition of machine tool that means the calculation or determination by tests the dynamic parameters involved in models.

The dynamic parameters, besides the mass ones, strongly influence the dynamic behavior of the assembly of servo axis and are a key element in defining the functional model. Figure 1 presents the structure of a feed drive of a machine tool along with the dynamic parameters required along each axis, stiffness k and damping d .

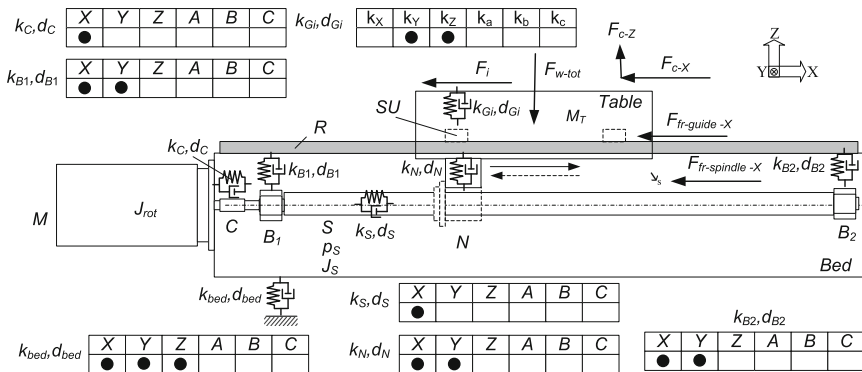


Fig. 1. Feed drive with stiffness and damping parameters of different subsystems and their significant components on axes.

There is a variety of bibliographic sources that propose on the basis of elaborated researches values of these parameters associated with different components in the kinematic chain.

3 Stiffness Modeling

In terms of stiffness, the modeling is characterized by two distinct levels: the model component and the stiffness and damping coefficients. For the first level, a modeling technique is used. In the second one, it is necessary to decide which coefficients and values have to be selected.

The stiffness coefficients of the linear guides, bas screws and nuts are derived from the catalog specifications. Rotational stiffness coefficients are not always available, and can be obtained on request from manufacturers. Some manufacturers use experimental stands to identify rigidity values of components. Other manufacturers focus on virtual calculation models to determine stiffness coefficients.

There is also a way that can be seen as the opposite, namely obtaining reliable information about the stiffness of the linear guides with intermediate elements or bearings by experimental identification that assumes that the tool machine is available for tests and there is also a model RBS or FEM, as demonstrated by numerous works in the field of machine tools [1, 15, 26, 30, 31].

3.1 Stiffness Modeling of Feed Drive

It is accepted that the static stiffness of a machine tool along an axis of the reference frame is variable for different positions occupied by the mobile element (mass of the machine) being influenced by:

- changes in contact stiffness caused by interferences of the mechanical interface (guides);
- backlash;
- dimensional changes of structural elements, such as the length of the screw deformed during the movement;
- position deviations of the component elements of the guides as a whole in the main directions of the reference system;
- preloading of bearings and guides.

If the clutch does not play an important role in the feed kinematic chain dynamics, then a dynamic scheme of the feed drive can be considered as Fig. 3 shows. The axial equivalent rigidity of the system can be determined with the general relation:

$$\frac{1}{k_e} = \sum_{i=1}^n \frac{1}{k_i}, \quad (1)$$

where k_e is the equivalent stiffness of the feed drive and k_i – component stiffness (k_{B1} , k_{B2} , k_S , k_N) (Fig. 2).

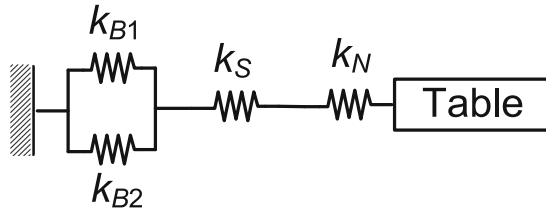


Fig. 2. Dynamic model with springs of the feed drive

Thus, for the case considered it is obtained:

$$\frac{1}{k_e} = \frac{1}{k_{Be}} + \frac{1}{k_S} + \frac{1}{k_N}, \text{ where } k_{Be} = k_{B1} + k_{B2}. \quad (2)$$

3.1.1 Method for Calculating the Ball Screw Stiffness

The stiffness of the ball screw can be determined by considering the screw as a bar loaded by an axial force that generates deformation. The mathematical relation of stiffness is the one known in the field of mechanics of materials [11]:

$$k_s = \frac{\pi d^2 E}{4l}, \quad (3)$$

where the bar is considered to have the diameter d (the smallest of the screw) and the length l . The quantity E is the elastic modulus of the screw material, usually steel ($E = 2.1 \cdot 10^{11} \text{ N/m}^2$).

The screw nut and mobile element of table type are considered to be halfway, which means that in most cases $l = L/2$, the spindle stiffness becoming

$$k_s = \frac{\pi d^2 E}{2L}. \quad (4)$$

Thus, the exact value of the length l for a certain position of the mobile element can be considered. In this case, it is possible to refer to the stiffness of the screw considering the whole length L , obtaining the relation:

$$k_s = \frac{\pi d^2 E}{2L} \cdot \frac{L}{l}. \quad (5)$$

3.1.2 Ball Screw Stiffness Given by Catalogues

The catalogues of ball screw nut components usually give information about this assembly type. The assembly stiffness is given by:

$$\frac{1}{k_{bs}} = \frac{1}{k_s} + \frac{1}{k_n}, \quad (6)$$

where k_{bs} is the total stiffness of the ballscrew [N/ μ m]; k_s – spindle stiffness [N/ μ m]; and k_n – nut stiffness [N/ μ m].

The spindle stiffness (see Eq. 4) depends on the assembly type:

$$k_s = 64.7 \frac{d_r^2}{L_1} \text{ for fixed - fixed assembly;} \quad (7)$$

$$k_s = 16.8 \frac{d_r^2}{L_1} \text{ for fixed - free assembly;} \quad (8)$$

For a single nut, the nut stiffness is:

$$k_n = 0.8 \times k \left(\frac{P}{0.1C} \right)^{1/3}, \quad (9)$$

where k is the stiffness in the table; P – preload; C – dynamic load on table.

3.1.3 Variable Ballscrew Stiffness

A linear axis of a milling machine, namely a feed drive is considered for the study. The slide is driven by a rotary motor and a ball screw-nut mechanism.

For a long ball screw of 1.5–2 m and more, its stiffness characteristic is variable. It is considered an initial length l_0 . The total stroke of the slide is h . The machining is done by a milling head and the cutting force component that is involved along the axis is the feed force F_{cut} as disturbance in the system.

In this case the screw stiffness becomes nonlinear due to the dependence of the elastic constant to the length according to (3):

$$k_{sx} = \frac{\pi d^2 E}{4l_x}, \quad (10)$$

where k_x is the ball screw stiffness, E – elasticity modulus of steel, $E = 2 \cdot 10^{11}$ N/m², A – screw cross section area, having expression $A = \frac{\pi d^2}{4}$; d – ball screw diameter in m.

The variable frequency ω_x of the system has the expression [25]:

$$\omega_x = \sqrt{\frac{EA}{m} \cdot \frac{1}{l_x}}, \quad (11)$$

where $l_x \in [l_0, l_0 + h]$.

If one considers an initial length $l_0 = 0.13$ m, for four ball screw sizes ($d_1 = 25$ mm, $d_2 = 40$ mm, $d_3 = 50$ mm, and $d_4 = 63$ mm) the variation of spindle stiffness with length for a total length of 2 m is presented in Fig. 3.

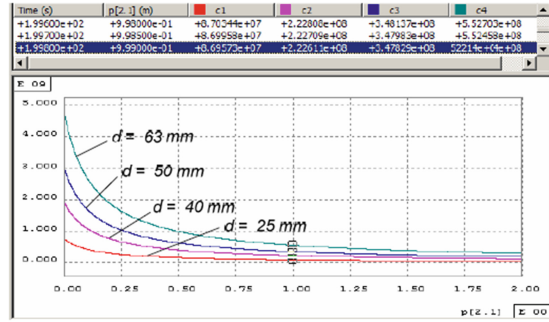


Fig. 3. Variation of ball screw stiffness with length [25]

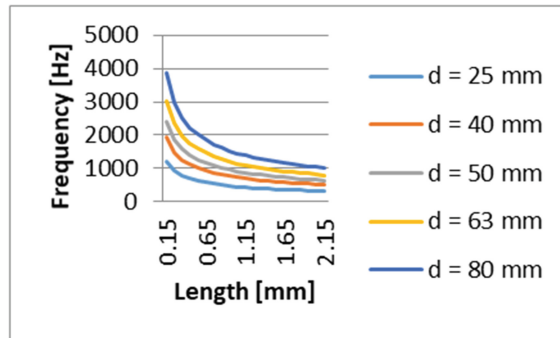


Fig. 4. Variation of ball screw frequency with stiffness and length.

The system frequency also is variable with regard to the active spindle length l_x . For the range of spindle diameters $d = [24; 40; 50; 63; 80 \text{ mm}]$ the variation is presented in Fig. 4. The mass is considered $m = 450 \text{ kg}$.

Wang et al. studied in [27] a CNC milling machine with three controlled axes X, Y, and Z, for which they calculated the stiffness of rolling joint (guide ways and ballscrew nut mechanism) along with the equivalent stiffness of the axes. The used values are given in Fig. 5 for having a global image of the feed drive dynamic definition.

Regarding the rolling guide stiffness calculated in work [27], the data grouped in Table 1 shows that there is a constant ratio between normal and tangential stiffness of $k_t/k_n = 0.71$. This ratio could be considered for calculating the tangential stiffness in which case the normal rigidity of the rolling guides is taken from catalogs.

3.2 Nut Stiffness

This is more than nut stiffness. It is the stiffness of the assembly spindle-balls-nut. It is obtained based on the Hertz contact theory, which implies three components: spindle through its thread groove, ball, and nut groove. The expression of the deformation of one ball becomes [27]:

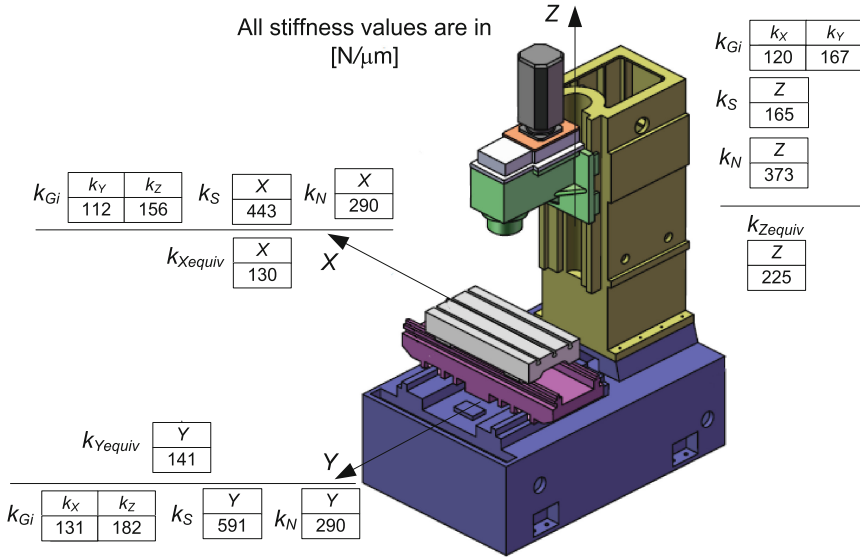


Fig. 5. Stiffness on milling machine axes calculated in work [27]

Table 1. Relation between normal and tangential stiffness

Normal stiffness of rolling guide k_n [N/mm]	Tangential stiffness of rolling guide k_t [N/mm]	Ratio k_t/k_n
167	120	0.718562874
156	112	0.717948718
182	131	0.71978022

$$\delta_i = \frac{K_i}{\pi a_i} \left[\frac{3P}{2} \left(\frac{1-u_1^2}{E_1} + \frac{1-u_2^2}{E_2} \right) \right]^{2/3} \left(\sum \rho_i \right)^{1/3}, i = 1, 2, \quad (12)$$

where P is the normal reaction on each ball; K_i and a_i – Hertz coefficients; β – pressure angle at contact ball-groove; δ_1 – deformation at contact ball-nut; δ_2 – deformation at contact ball-screw; E_1 and E_2 – moduli of elasticity of the two contact components; u_1 and u_2 – Poisson coefficients of the contact objects; $\sum \rho$ – synthetic curvature at contact point.

The synthetic curvature for the contact points ball-nut (1) and ball-screw (2) are respectively:

$$\sum \rho_1 = \frac{2}{d_b} + \frac{2}{d_b} - \frac{1}{d_b f_1} - \frac{2 \cos \alpha \cos \phi}{d + d_b \cos \alpha}, \quad (13)$$

$$\sum \rho_2 = \frac{2}{d_b} + \frac{2}{d_b} - \frac{1}{d_b f_2} - \frac{2 \cos \alpha \cos \phi}{d + d_b \cos \alpha}, \quad (14)$$

where d_b is the ball diameter; f_1 – form factor as ratio nut groove radius to ball radius; f_2 – form factor as ratio screw groove radius to ball radius.

The axial deformation of nut against spindle is:

$$\delta_N = (\delta_1 + \delta_1) / \sin \beta \cos \phi, \tag{15}$$

leading to the nut stiffness k_N

$$k_N = F_a / \delta_N, \tag{16}$$

where F_a is the preload force in screw-nut assembly that at static equilibrium gives the equation:

$$F_a - Pz \sin \beta \cos \phi = 0, \tag{17}$$

with z the number of balls; ϕ – lead screw angle; P – normal reaction of each ball.

The assembly ball screw nut rigidity according to [28] is as follows:

$$k_N = \frac{1}{3\pi} \left[\frac{3}{2} \left(\frac{1 - \mu_1}{E_1} + \frac{1 - \mu_2}{E_2} \right) \right]^{\frac{2}{3}} \left[\frac{K_n(e)}{m_{na}} \left(\sum \rho_n \right)^{\frac{1}{3}} + \frac{K_s(e)}{m_{sa}} \left(\sum \rho_s \right)^{\frac{1}{3}} \right] Z^{\frac{2}{3}} (\sin \beta)^{\frac{5}{3}} (\cos \lambda)^{\frac{1}{3}} F_p^{\frac{1}{3}}, \tag{18}$$

where E is the Young’s modulus, μ – Poisson’s ratio, F_p – the preload of gasket, Z – ball number, λ – helix angle, β – contact angle.

From the product catalog [21], data on the stiffness of nuts with various nominal dimensions of the threaded part can be obtained (Fig. 6).

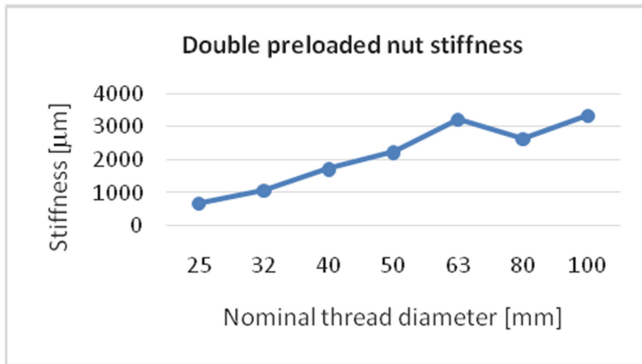


Fig. 6. The influence of nominal diameter on the stiffness of double-nut screw [21].

From the catalog values it is found that for the same nominal diameter d the stiffness is higher for the smaller step (which means a smaller angle of the helix). For example, in the catalog [21], for a diameter of 40 mm, there are two values of 1710 N/μm ($p = 10$ mm) and 1030 N/μm ($p = 20$ mm) in ratio $r = 1.66$. For the same nominal diameter, the ratio is variable because the variants are different in terms of the number of ball circuits and sometimes the diameter of the ball, etc.

3.3 Influence of Bearing Stiffness

The following are some theoretical and practical methods for determining the bearing stiffness with application to angular contact ball bearing. Methods are compared in order to provide an image of methods in order to choose the stiffness values for a dynamic application.

From a theoretical perspective, bearing stiffness is a relation that is based on the contact between the rolling element (ball or roller) and the inner ring.

Obviously, it depends on the material (usually steel on steel or ceramic on steel contact) and also the geometric parameters and the number of rolling elements [2].

Radial stiffness of the bearing is given as the ratio between the force F_r and deflection δ_r , by:

$$k_r = \frac{F_r}{\delta_r}. \tag{19}$$

Paper [1] gives the following expression of radial stiffness:

$$k_r = c_{type} \frac{(D + d)^{2/3}}{(D - d)^{1/4}} F_r^{1/3}, \tag{20}$$

where: D – external diameter of the bearing [mm]; d – inner diameter [mm]; F_r – radial component of the cutting force (F_x) [N]; c_{type} – coefficient of the bearing type including the influence of the contact angle α (Table 2); α – contact angle (for series A $\rightarrow 25^\circ$, C $\rightarrow 15^\circ$).

The bearing deformation can be calculated according to [17]:

$$\delta = kF^p, \tag{21}$$

where: k is the coefficient of proportionality; F – force on bearing [N]; p – exponent: 2/3 for ball bearings, 2/3–9/10 for roller bearings.

Thus, the bearing stiffness becomes:

$$c = F/\delta = F^{1-p}. \tag{22}$$

Table 2. Values of the bearing type coefficient

Series type	719...C	719...AC	70...C	70...AC	72...C	72...AC
c_{type}	4.83	5.83	5.43	6.03	5.38	6.03

The ball bearing deformation is a function of external force:

$$\delta_r = \frac{k}{\cos \alpha} \sqrt[3]{\frac{Q^2}{D_w}}, \text{ where } k = 0.436, \tag{23}$$

with deformation given by expression:

$$\delta_r = \left[10^{-4} \cdot \frac{0.002}{(\cos \alpha)^{2/3}} \left(\frac{5}{10} \right)^{2/3} \right] F_r^{2/3} \cdot d_b^{1/3} (i \cdot n)^{2/3}. \tag{24}$$

The Krämer method proposes an expression of rigidity given by

$$k_r = \frac{nF_r}{x_r}, \tag{25}$$

where the deformation for ball bearings is calculated with relation

$$x_r = 1.2 \times 10^{-7} \times d_b^{-1/3} \times Z^{-2/3} \times F_r^{2/3}, n = 3/2. \tag{26}$$

Three dimensional angular contact ball bearings were considered for calculation, namely type 7012 ($d = 60$ mm, $D = 95$ mm), 7017 ($d = 85$ mm, $D = 130$ mm), 7018 ($d = 90$ mm, $D = 140$ mm).

Radial stiffness variation diagrams through method [2] are shown in Fig. 7, through Palgrem method [17] in Fig. 8, and Krämer method [14] in Fig. 9.

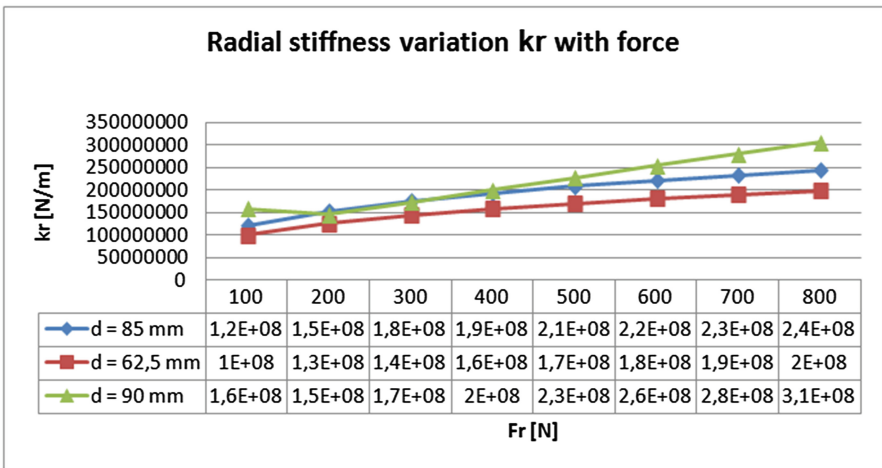


Fig. 7. Diagram of radial stiffness variation for angular contact ball bearing type 70...C after [17]

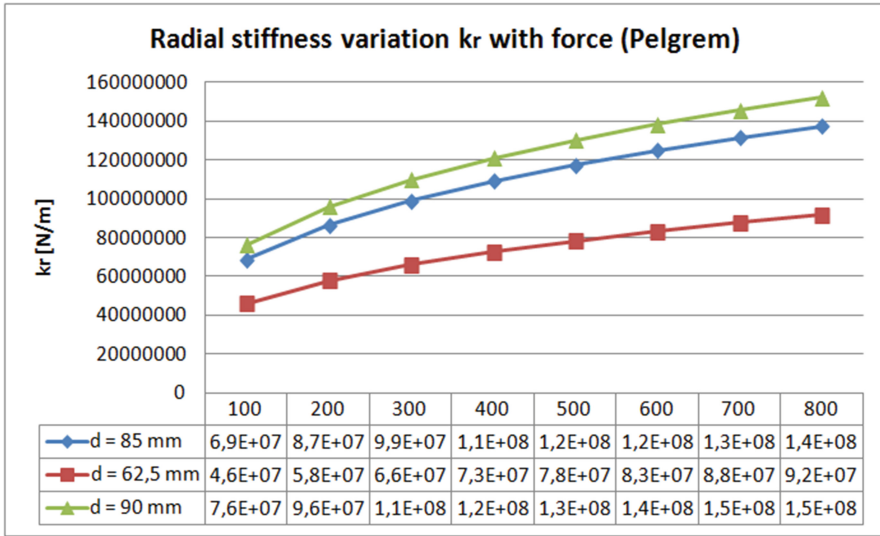


Fig. 8. Diagram of radial stiffness variation for angular contact ball bearing type 70...C after [17]

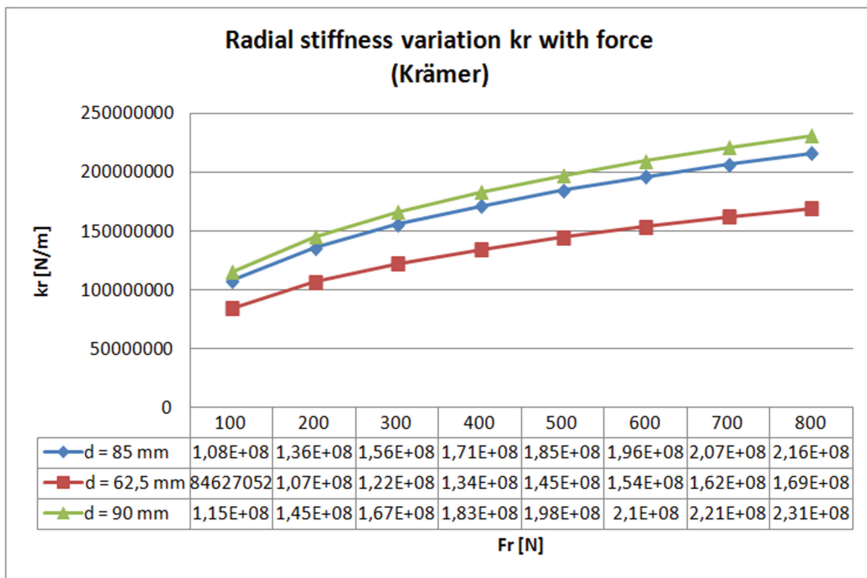


Fig. 9. Diagram of radial stiffness variation for angular contact ball bearing type 70...C after [14]

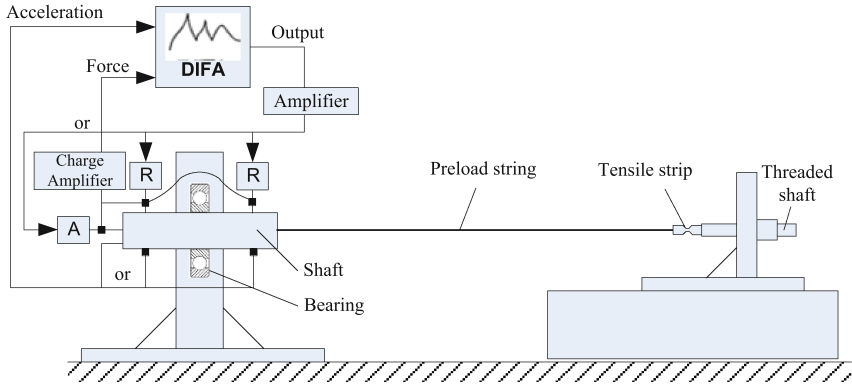


Fig. 10. The measurement diagram of the transfer function [13]

3.3.1 Relationship Between Axial and Radial Stiffness of Bearings Given by Design Experience

In modeling ball bearings, especially in angular contact ball bearings, the following relationships between the radial and axial stiffness are used:

$$k_r = k_a/2 \cdot \cot g^2 \alpha, \quad (27)$$

where α is the contact angle.

3.3.2 Bearing Stiffness Given by Product Catalogs

The bearing catalogs of the manufacturing companies offer relations based on experimental data of radial and axial stiffness that are customized with values specific to each type of bearing, size, load, etc.






The bearing catalog [12] gives the axial rigidity c_a for bearing pairs in an O or X arrangement in tables. It supplies also the relation between radial rigidity c_r and the axial one c_a :

- $c_r = 6 \cdot c_a$ for $\alpha = 15^\circ$,
- $c_r = 3.5 \cdot c_a$ for $\alpha = 20^\circ$,
- $c_r = 2 \cdot c_a$ for $\alpha = 25^\circ$,

where α is the contact angle.

To determine the axial stiffness, the bearing has to be preloaded. The lift-off force up to which the deflection is almost linear is shown in Table 3 along with the axial stiffness c_a of the bearing sets.

Table 3. Axial rigidity for different bearing arrangements [12]

Bearing arrangement	Axial rigidity c_a [N/ μm]	Lift-off force K_{aE} [N]
	c_a	$3F_v$
	$1.64 c_a$	$6F_v$
	$2 c_a$	$6F_v$
	$2.24 c_a$	$9F_v$
	$2.64 c_a$	$9F_v$

The axial rigidity is given by the catalog for three cases of preloading: L – low, M – medium; H – high. Table 4 presents axial rigidity ranges for different angular contact bearing series and sizes (d – bearing bore diameter [mm]).

Table 4. Rigidity ranges for angular contact bearings (after [12])

d	Axial rigidity c_a [N/ μm]		
	L	M	H
10	8.8-35.8	14.1-63.2	19.6-88.8
12	9.4-42.8	15-66.8	20.8-103.1
15	11.4-49.7	18.2-84.4	25.2-117.3
17	17-53.3	19.2-89.9	26.5124.6
20	15-63.7	23.7-106	32.7-146.7
25	17-69.2	26.8-115.2	36.9-158.8
30	21.3-90.4	34.8-148.3	44.5-203.3
35	24.5-103.2	38.6-169.4	53-232.2
40	26.6-113.5	41.8-184.3	57.2-251.6
45	30.8-120.8	48.4-196.1	66.2-267.8

d	Axial rigidity c_a [N/ μm]		
	L	M	H
50	32.6-138.3	51.2-222.9	70-303.3
55	37.3-154.6	58.6-249.2	80.3-338.8
60	39.5-164.9	62.2-264.1	85-358.3
65	41.5-184.8	65-294.5	88.8-399
70	47-193.7	73.7-308.6	100.6-417.8
75	49.5-203.8	77.5-324.7	105.7-439.4
80	52.3-220.9	81.9-399.3	111.7-471.6
85	55.9-233.1	87.4-368.5	118.9-497.4
90	57.2-257.1	89.4-404.3	121.6-544.6
95	60-272.7	93.7-428.7	127.4-577.3

3.3.3 Experimental Determination of Bearing Stiffness

The experimental determination of the stiffness of bearings used for shaft-bearing assemblies is a tool used for correcting the theoretical models and for assessing the usefulness of the models for estimating the behavior of the shaft-bearing assembly on vibration.

Certainly, experimental assemblies used to determine the rigidity of bearings are based on axial or radial loading with increasing forces in a range and the measurement of displacements in axial or radial directions, respectively.

Knappen proposes in work [13] an experimental stand that is dynamically excited with an exciting hammer or shaker to determine the transfer matrix of the bearing. The preloaded bearing is considered because the non-preloaded bearings are difficult to estimate. Figure 10 presents several solutions of experimental stands that have various

advantages and disadvantages. It is considered to be more suitable for experimental tests the stand after Heuvelmans used to determine the linear and rotational stiffness of the bearing (Fig. 10). Preloading is measured by a tensile strip. Measurement of the transfer is done through the Dynamic Signal Analyzer - DIFA, represented in Fig. 10. Two R excitators controlled by DIFA load the shaft in a radial direction. In axial load only the excitator A is used. Both force and acceleration are measured and taken over by DIFA.

It starts from the general dynamic equation and uses identification algorithms that use the Least Square Algorithm to minimize the fit error:

$$\underline{M}\ddot{q} + \underline{B}\dot{q} + \underline{K}q = f, \tag{28}$$

$$\underline{A}^T \underline{A} \hat{X}_{ls} = \underline{A}_T \underline{E}, \tag{29}$$

where \underline{A} and \underline{E} contain model characteristics and experimental data. \hat{X}_{ls} contains the unknowns of the dynamic equation.

The differences between the measured and modeled values are made by an iterative solving algorithm:

$$\underline{V}^T \underline{A} \hat{X}_{iv} = \underline{V}^T \underline{E}, \tag{30}$$

where the \underline{V} matrix contains variable instrumental outputs.

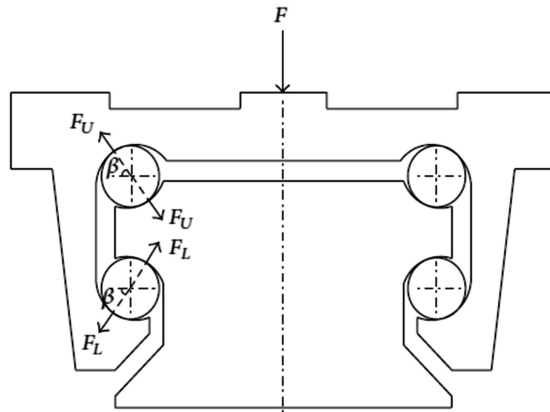


Fig. 11. Force acting on rolling guide joint [27]

3.4 Guideways Stiffness

3.4.1 Linear Rolling Guide Model

The calculation of rigidity of linear guides with intermediate elements is the same as that of ball nut or bearings based on Hertz's theory. The expression of the deformation of one ball given by [27] on the basis of [32] has the same form as (12). $\sum \rho$ is the

synthetic curvature at contact point; namely, $\sum \rho = \sum_{i=1}^2 \sum_{j=1}^2 (1/R_{ij})$, where R_{ij} ($i = 1, 2; j = 1, 2$) are principal curvatures of the object \underline{V}_i .

The rolling guide block-balls-rail is shown in Fig. 11. There are four balls in joint, total number of one row balls being \ddagger , and contact angle ball-groove is β . The force F generates a normal reactions F_U on the upper row and F_L on the lower row. The equilibrium equation on normal direction is:

$$F + xF_L \sin \beta/2 = zF_U \sin \beta/2. \quad (31)$$

The relation between the preload force and the force distributed on the ball is:

$$F_0 = \sqrt{2}zP_0 \sin \beta. \quad (32)$$

The upper displacement δ_U and the lower one δ_L define the displacement on normal direction δ_n :

$$\delta_n = (\delta_U - \delta_0) \sin \beta = (\delta_0 - \delta_L). \quad (33)$$

where initial deformation δ_0 is given by (12).

The normal stiffness of the guide unit is

$$K_n = F \cdot \delta_n. \quad (34)$$

The lateral displacement without additional force is $\delta_r = (\delta_U - \delta_0) \cos \beta$ leading to the tangential stiffness of the guide

$$K_t = zP_0 \cos \beta/2 \cdot \delta_r. \quad (35)$$

3.4.2 Stiffness Given by Catalogues

Mathematical way of stiffness determinations is time consuming. It is not independent of the product catalogues because it needs dimensions, numbers and materials. Therefore, for an immediate solution for guideway stiffness for modeling feed drives, the catalogues could be employed. For example, the catalogue [10] gives information for guideways types and load category.

With regard to the preload case of linear guides, for machine tools three classes are of interest:

- medium preload (Z2, specific to Z axis for general industrial machines, EDM, NC lathes, precision X-Y tables, measuring equipment);
- heavy preload (Z3, specific to machining centers, grinding machines, NC lathes, horizontal and vertical milling machines, Z axis of machine tools);
- super heavy preload (Z4, specific to heavy cutting machines).

Some recommendation for stiffness values to be used in modeling applications are given in Figs. 12 and 13 considering different dimensions of the rail width in the range [15, 20, 25, 30, 35, 45, 55, 65 mm] based on catalog [10].

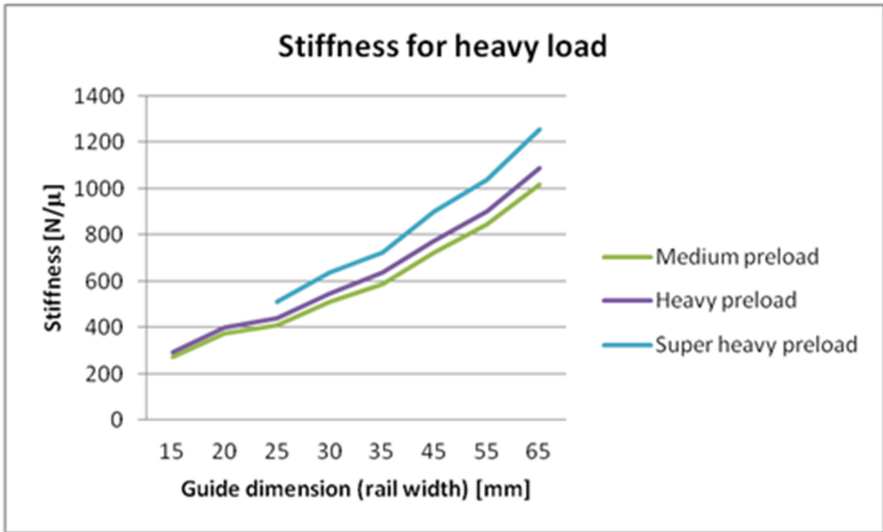


Fig. 12. Linear guide stiffness recommendations for heavy load

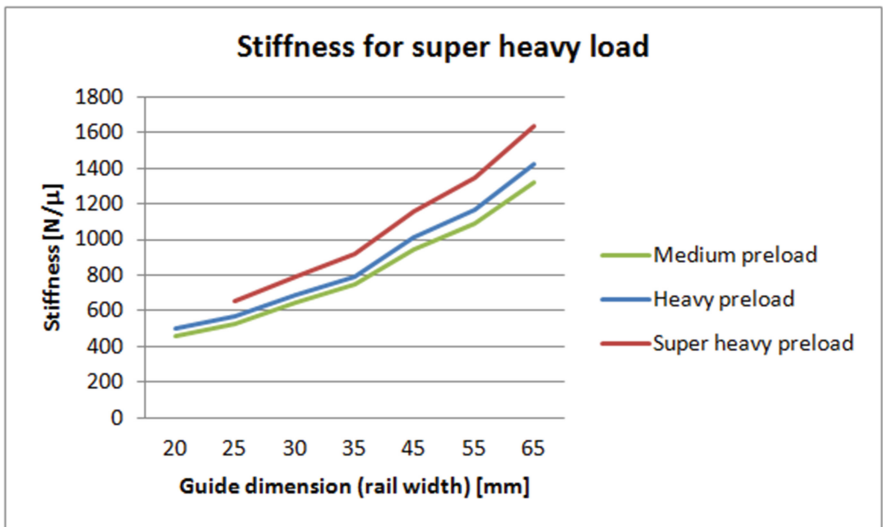


Fig. 13. Linear guide stiffness recommendations for super heavy load

4 Damping Modeling

There are three important sources of damping in mechanical systems, namely:

- structural damping inside the material;
- damping in the joints;
- damping at certain points in the structure that is not well known.

Structural damping is generated inside the material and is caused by the effects of internal friction that produces internal energy dissipation with deformation of components during vibration. Material is a determining factor in this situation and will greatly influence the behavior of machine tools.

The most used materials for the structural elements of machine tools (beds, columns, traverses, etc.) are:

- steel and cast iron;
- welded steel and iron cast structures with lower damping capacity;
- granite;
- alternative materials such as polymer concrete for massive fixed structures of machine tools.

Dynamic equation of the system

$$m\ddot{x} + d\dot{x} + kx = 0. \quad (36)$$

has the characteristic equation $ms^2 + ds + k = 0$ has the solution of the form:

$$x = e^{t \left(\frac{-d}{2m}\right)} \left[A e^{t \left[\left(\frac{d}{2m}\right)^2 - \frac{k}{m}\right]^{1/2}} + B e^{-t \left[\left(\frac{d}{2m}\right)^2 - \frac{k}{m}\right]^{1/2}} \right], \quad (37)$$

where A and B are arbitrary constants that depend on the initial conditions.

The critical damping coefficient is:

$$d_c = 2\sqrt{mk} = 2m\omega_0. \quad (38)$$

where ω_0 is the natural frequency of the system. The damping ratio is given by the ratio between real and critical damping:

$$\zeta = \frac{d}{d_c} = \frac{d}{2\sqrt{mk}} = \frac{\Lambda}{2\pi} = \frac{\delta}{\omega} = \frac{\eta}{2}, \quad (39)$$

where: d – damping coefficient; m – mass; k – stiffness; Λ – logarithmic decrement; δ – depreciation constant; ω – angular frequency; η – the loss factor.

Table 5 shows values of the damping ratio relevant to machine tool structures [16].

Table 5. Damping ratios for machine structures [16]

Material	Damping ratios
Steel	0.001–0.002
Cast iron	0.002–0.004
Polymer concrete	0.02–0.0
Welded structure	0.004–0.08
Bed	0.04–0.08

Joint damping of the joints results from the energy dissipation that takes place in the machine parts in contact with the moving parts, such as linear guides, bearings, ball screw nuts, whose operation is based on rolling elements (balls or rollers). These sources are multiple and change the way of approaching damping within a complex machine-tool system.

Table 6 shows values for bearing used for rotation axes and main shafts indicated by the paper [20], which shows a retrospective of the damping parameters for different components of machine tools. Regarding the linear guides, the paper [9] highlights the influence of the experimental results on the identification of the damping parameters (Table 7).

The friction moment in bearing has two distinct components, one involving the viscosity of the lubricant and the speed of rotation, and the second one involving the effect of the loading in the bearing (Table 8):

$$Mr = 10^{-7}f_0(v \cdot n)^{2/3}d_m^3 + f_1P_1d_m. \tag{40}$$

The relation is used for $v \cdot n \geq 2000$, where: Mr is the friction torque [Nmm]; v – kinematic viscosity at working temperature [mm²/s]; n – speed [min⁻¹]; P_1 – equivalent load on bearing [N]; d_m – average diameter $(d + D)/2$ [mm] with inner diameter d and outer diameter D ; f_0 and f_1 – lubrication and time dependent coefficients [–] in reference with [DIN ISO 15312].

Table 6. Damping values for bearings [20]

Component	Damping ratios
Bearings (inner diameter 55 mm)	2 000–9 000 Ns/m
Bearings (inner diameter 90 mm)	5 500–12 000 Ns/m
Bearings (inner diameter 120 mm)	50 000–550 000 Ns/m
Bearings (inner diameter 160 mm)	200 000–1 000 000 Ns/m

Table 7. Damping values for linear guides [9]

Component	Damping value
Ball linear guideway (rail size 35 mm)	4 000–10 000 Ns/m
Roller linear guideway (rail size 35 mm)	3 500–14 500 Ns/m
Ball linear guideway (rail size 45 mm)	4 000–14 000 Ns/m
Roller linear guideway (rail size 45 mm)	6 500–10 500 Ns/m

It is noted that the first term depends on the speed that for feed drives is variable and therefore a specific value for modeling could not be chosen, the process becoming one complex for machine tools. The speed is variable from low (even zero) values, where strong nonlinear phenomena such as stick-slip and hysteresis phenomena may occur, up to values close to the maximum.

Complexity may also increase if loading on bearings or linear guides with rolling elements is considered variable. This can be caused by the continuous change in the position of the center centers, inertial loads produced by the acceleration of the axes, and additional stresses introduced by the forces from the cutting process. Taking them into consideration can cause the friction caused by the instantaneous load not to be determined.

Even if the behavior is speed dependent, it is relatively linear for speeds in the range of 5 000–40 000 mm/min, low speed zone remaining highly complex (Table 9).

Table 8. Friction coefficients for bearing [23]

Component	f_{0r}	f_{1r}
Deep groove ball bearing	1.7–2.3	0.00010–0.00020
Self-aligning ball bearing	2.4–4	0.00008
Angular contact ball bearing	2–7	0.00025–0.00035
Four point bearing	2–3	0.00037
Cylindrical roller bearing with cage	2–4	0.00020–0.00040
Cylindrical roller bearings full complement	5–12	0.00055
Needle-roller bearing	5–10	0.00050
Self-aligning roller bearing	4.5–6.5	0.00017–0.00036
Tapered roller bearing	3–4.5	0.00040
Axial cylinder roller bearing	3–4	0.00150
Axial self-aligning roller bearing	2.5–3.3	0.00023–0.00033

Table 9. Friction coefficients at different force levels for linear guides [16]

Component	Friction force			
	0 kN	10 kN	20 kN	30 kN
$v = 5\ 000\ \text{mm/min}$				
Ball linear guideway (35 mm)	15–20 N	30–35 N	50–55 N	95–100 N
Roller linear guideway (35 mm)	30–35 N	40–45 N	45–50 N	55–60 N
Ball linear guideway (45 mm)	25–30 N	40–45 N	65–70 N	100–105 N
Roller linear guideway (45 mm)	65–70 N	65–70 N	75–80 N	85–90 N
$v = 40\ 000\ \text{mm/min}$				
Ball linear guideway (35 mm)	30–45 N	40–55 N	60–75 N	100–115 N
Roller linear guideway (35 mm)	55–70 N	55–70 N	65–80 N	70–85 N
Ball linear guideway (45 mm)	45–60 N	55–70 N	70–85 N	105–120 N
Roller linear guideway (45 mm)	125–140 N	125–140	130–145 N	135–150 N
Guideway wipers	10–40 N			

As regards other damping sources, they manifest themselves in certain points of the structure of the machine where the energy dissipation occurs, points not so well known and therefore they are included in material damping or even ignored.

5 Determination of Dynamic Parameters of Feed Drives

5.1 Static Stiffness Measurement

The classic method of determining static stiffness is not standardized being just recommended. In most cases, it is minimalist, being made in one point (position of the mobile element) by loading the mobile element with a certain force in the positive and then negative direction of the axes. Practically, it provides only one single-point rigidity value in the XOY plane.

There are large significant differences between the static stiffness measured by the classical method and that obtained by other methods. One method is proposed by Tomáš Stejskal et al. [24] in which the measurements are made immediate after machine stop, in a certain number of points.

In the first method (Fig. 14a), the measurements are made in a number of points (up to 9) evenly displaced along studied axis. For each point, the measurement of displacement is made for a load F which is gradually increased in a range F_1 – F_8 . Then the measurements are done for a load decreased belonging to the same range.

The second procedure considers measurements from the first position to the last one and back to position 1. The first cycle consists of 1-9-1 displacement without load ($F = 0$ N) and a repeated cycle with a load $F_1 \neq 0$. After the first cycle, the second one is considered with increased load force $F_2 > F_1$.

In the third approach (Fig. 14b), several measurements are made for a load F in each point and also in proximity of the point, moving the slide alternatively in positive and negative direction with a small distance ($l = 5$ mm) (Fig. 14c).

The cycle continues repeating the measurements for an increased force form the range. Then, the slide is moved to the next point resuming the measurement cycle.

The loading force could be considered in the range [20; 40; 60; 80; 100; 120; 140; 160 N].

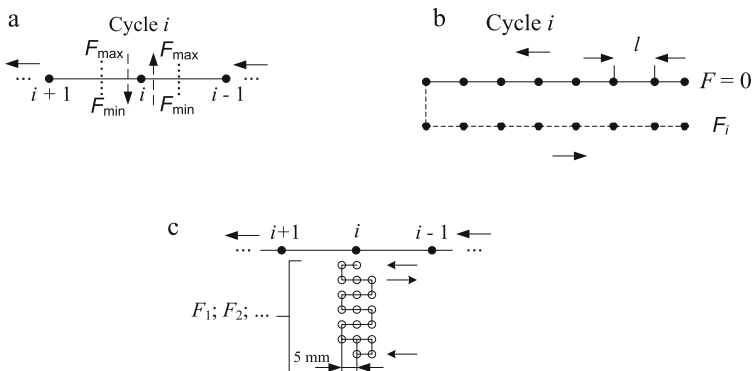


Fig. 14. Measurement methods of the total stiffness of the feed drive [24]

5.2 Dynamic Characteristic Identification

Modeling is a difficult task, especially when trying to consider both linear and rotary motions of the system with dynamic characteristics (stiffness, damping and friction). In DBS, the mathematical processing is complex, the model being very sensitive when introducing the variable position as a time dependent one $x(t)$, $y(t)$, and $z(t)$.

Some applications require the system modeling as a transfer function. The order n plays a very important role due to the fact that reduced orders ($n = 1; 2$) lead to a model accuracy of 70–80%. A greater precision is obtained for increased orders. For instance, the dynamic stiffness of the feed drive in the work [18] has the form:

$$Sd(s) = \frac{F(s)}{Xo(s)} = \frac{a_5s^5 + a_4s^4 + a_3s^3 + a_2s^2 + a_1s + a_0}{b_3s^3 + b_2s^2 + b_1s + b_0}, \quad (41)$$

in which all coefficients are defined by relations depending on system parameters.

This model including dynamic stiffness is very complex and the definition of all parameters becomes a difficult challenge. This is achieved on the bases of experimental measurements. Based on them, some algorithms of identification available in specific programs are used.

6 Conclusions

The paper has emerged from the need to gather together some concepts related to the modeling of the kinematic chains of the machine tools, which influence decisively the precision of machining.

Methods of determining of dynamic characteristics by mathematical calculations, through measurements, or based on product catalog information, are presented. Values or ranges of the values specific to some components and applications as well as some values specific to some research are presented.

In addition to the dynamic parameters of the feed drive components, some theoretical and experimental methods of setting of stiffness and damping of the feed drive assembly are presented.

Particular aspects related to the dynamic characteristics of feed drives may also be revealed. Thus, the stiffness of the preloaded ball nut is revealed not to vary with loading. It results that, in order to increase the rigidity of the assembly, the rigidity of the bearings can be considered by increasing their number in the arrangement. Also, one can choose a larger diameter of the ball screw.

References

1. Ahmadi, K., Ahmadian, H.: Modelling machine tool dynamics using a distributed parameter tool–holder joint interface. *Int. J. Mach. Tools Manuf* **47**(12–13), 1916–1928 (2007)
2. Butcher, E.A., Nindujarla, P., Bueler, E.: Stability of up-and down-milling using Chebyshev collocation method. In: ASME 2005 International Design Engineering Technical Conferences and Computers and Information in Engineering Conference, pp. 841–850. American Society of Mechanical Engineers, January 2005

3. Constantin, G., Ghionea, A.: Feed kinematic chain of the bridge in Gantry machine-tools. *Archiwum Technologii Maszyn i Automatykacji* **28**(2), 75–84 (2008)
4. Constantin, G., Predincea, N.: Aspectes regarding optimal design of machine tool feed drives. *Proc. Manuf. Syst.* **10**(4), 171 (2015)
5. Copani, G., Molinari Tosatti, L., Lay, G., Schroeter, M., Bueno, R.: New business models diffusion and trends in European machine tool industry. In: *Proceedings of 40th CIRP International Manufacturing Systems Seminar*, May 2007
6. Erkorkmaz, K., Yeung, C.H., Altintas, Y.: Virtual CNC system. Part II. High speed contouring application. *Int. J. Mach. Tools Manuf.* **46**(10), 1124–1138 (2006)
7. Fleischer, J., Broos, A.: Parameteroptimierung bei Werkzeugmaschinen—Anwendungsmöglichkeiten und Potentiale. *Weimarer Optimierungs-und Stochastiktage*, 1 (2004)
8. Fredin, J.: *Modelling, simulation and optimisation of a machine tool* (Doctoral dissertation, Blekinge Institute of Technology) (2009)
9. Groche, P., Hofmann, T.: Einfluss des dynamischen Übertragungsverhaltens von Stoßführungen auf die Arbeitsgenauigkeit von Umformpressen. *EFB Hannover* (2005)
10. HIWIN Linear Guideway. [http://ruchservomotor.com/Pdf_english/H_L_G_\(Low\).pdf](http://ruchservomotor.com/Pdf_english/H_L_G_(Low).pdf)
11. HIWIN Ballscrews. Technical Information. <https://www.hiwin.com/pdf/ballscrews.pdf>
12. INA-FAG, Schaeffler Technologies, Super Precison Bearings (2006). https://www.schaeffler.com/remotemedien/media/_shared_media/08_media_library/01_publications/schaeffler_2/catalogue_1/downloads_6/sp1_de_en.pdf
13. Knaapen, R.J.W., Kodde, L., de Kraker, A.: *Experimental Determination of Rolling Element Bearing Stiffness*. Technische Universiteit Eindhoven, Eindhoven (1997)
14. Krämer, E.: *Dynamics of Rotors and Foundation*. Springer, Berlin (1993)
15. Lee, W.J., Kim, S.I.: Joint stiffness identification of an ultra-precision machine for machining large-surface micro-features. *Int. J. Precis. Eng. Manuf.* **10**(5), 115–121 (2009)
16. Maglie, P.: *Parallelization of Design and Simulation*, vol. 683. ETH Zurich, Zürich (2012)
17. Palmgren, A.: *Les Roulments, Description, Theorie, Applications* (Bearings, Description, Theory, Applications). SKF, Paris (1967)
18. Pandilov, Z., Milecki, A., Nowak, A., Górski, F., Grajewski, D., Ciglar, D., Klaić, M., Mulc, T.: Virtual modelling and simulation of a CNC machine feed drive system. *Trans. FAMENA* **39**(4), 37–54 (2015)
19. Riba, R.C., Pérez, R.R., Ahuett, G.H., Jorge, L.S.A., Domínguez, M.D., Molina, G.A.: Metrics for evaluating design of reconfigurable machine tools. In: *International Conference on Cooperative Design, Visualization and Engineering*, pp. 234–241. Springer, Berlin, Heidelberg, September 2006
20. Schlecht, B.: *Maschinenelemente: Getriebe-Verzahnungen-Lagerungen*. Pearson Studium, ein Imprint von Pearson Education (2010)
21. Servomech, Ball screws and nuts, Catalogue (2010). <http://www.servomech.it/Pdf/prodotti/SERVOMECH-ball-screws-and-nuts-catalogue.pdf>
22. Slocum, A.: *Precision Machine Design*. Society of Manufacturing Engineers, Dearborn (1994)
23. Steinhilper, W., Sauer, B., Feldhusen, J.: *Konstruktionselemente des Maschinenbaus 1: Grundlagen der Berechnung und Gestaltung von Maschinenelementen*. Springer, Heidelberg (2008)
24. Stejskal, T., Svetlík, J., Dovica, M., Demeč, P., Král, J.: Measurement of static stiffness after motion on a three-axis CNC milling table. *Appl. Sci.* **8**(1), 15 (2017)
25. Stratulat, F., Ionescu, F., Constantin, G.: Dynamic evaluation of a linear axis in milling using modelling and simulation environment. In: *Proceedings of the International Conference on Manufacturing Systems, ICMaS*, pp. 99–104 (2007)

26. Thurneysen, M., Demaurex, G.: Modalanalyse von komplexen Maschinen, praktische Ueberpruefung. In: Symposium Simulation von Werkzeugmaschinen. IWF/inspire, ETHZ (2008)
27. Wang, D., Lu, Y., Zhang, T., Wang, K., Rinoshika, A.: Effect of stiffness of rolling joints on the dynamic characteristic of ball screw feed systems in a milling machine. *Shock Vib.* **2015**, 11 (2015)
28. Xian-chun, S., Jian, S., Ming-yuan, C., Yan-feng, L.: Research on axial stiffness of the double-nut ball screw mechanism. In: Proceedings of the 1st International Conference on Mechanical Engineering and Material Science. Atlantis Press, December 2012
29. Zaeh, M., Siedl, D.: A new method for simulation of machining performance by integrating finite element and multi-body simulation for machine tools. *CIRP Ann. Manuf. Technol.* **56**(1), 383–386 (2007)
30. Zaghbani, I., Songmene, V.: Estimation of machine-tool dynamic parameters during machining operation through operational modal analysis. *Int. J. Mach. Tools Manuf* **49**(12–13), 947–957 (2009)
31. Zhang, Y.M., Xie, Z.K., Liu, Y.X.: Modeling and calculation of dynamic performances of NC machine tool considering linear rolling guideway. *Appl. Mech. Mater.* **16**, 510–514 (2009)
32. Zhu, J., Zhang, T., Li, X.: Dynamic characteristic analysis of ball screw feed system based on stiffness characteristic of mechanical joints. *J. Mech. Eng.* **51**, 72–82 (2015)